

Role of Hydrophobic Interactions in Binding *S*-(*N*-Aryl/*N*-alkyl-*N*-hydroxycarbamoyl)glutathiones to the Active Site of the Antitumor Target Enzyme Glyoxalase I

Avinash Kalsi, Malcolm J. Kavarana, Tianfen Lu, Dale L. Whalen, Diana S. Hamilton,* and Donald J. Creighton*

Department of Chemistry and Biochemistry, University of Maryland, Baltimore County, 1000 Hilltop Circle, Baltimore, Maryland 21250

Received April 6, 2000

Hydrophobic interactions play an important role in binding *S*-(*N*-aryl/*N*-alkyl-*N*-hydroxycarbamoyl)glutathiones to the active sites of human, yeast, and *Pseudomonas putida* glyoxalase I, as the log K_i values for these mechanism-based competitive inhibitors decrease linearly with increasing values of the hydrophobicity constants (π) of the *N*-aryl/*N*-alkyl substituents. Hydrophobic interactions also help to optimize polar interactions between the enzyme and the glutathione derivatives, given that the K_i value for *S*-(*N*-hydroxycarbamoyl)glutathione ($\pi = 0$) with the human enzyme is 35-fold larger than the interpolated value for this compound obtained from the log K_i versus π plot. Computational studies, in combination with published X-ray crystallographic measurements, indicate that human glyoxalase I binds the syn-conformer of *S*-(*N*-aryl-*N*-hydroxycarbamoyl)glutathiones in which the *N*-aryl substituents are in their lowest-energy conformations. These studies provide both an experimental and a conceptual framework for developing better inhibitors of this antitumor target enzyme.

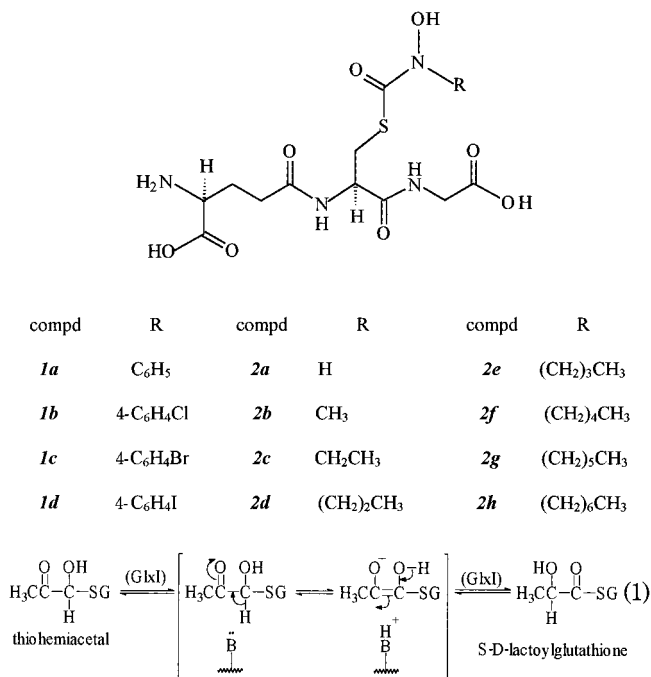
Introduction

The glyoxalase enzyme system has been the focus of much recent attention as a potential target for antitumor drug development.^{1,2} This enzyme system, composed of the isomerase glyoxalase I (GlxI) and the thioester hydrolase glyoxalase II (GlxII), promotes the glutathione (GSH)-dependent conversion of cytotoxic methylglyoxal to D-lactate.^{3,4} The toxicity of methylglyoxal, a byproduct of normal cellular metabolism,⁵ appears to arise from its ability to cross-link proteins and to form adducts with DNA.^{6,7} We recently demonstrated that selected *S*-(*N*-aryl-*N*-hydroxycarbamoyl)glutathiones **1a–c** (Chart 1, Table 1) are powerful competitive inhibitors of human GlxI^{8,9} and that the [*glycyl,glutamy*]diethyl ester prodrugs inhibit the growth of both murine and human tumors in vitro¹⁰ and in vivo.¹¹ Tumor toxicity appears to be due to inhibition of intracellular GlxI, which results in elevated levels of methylglyoxal.¹⁰ Thus, GlxI appears to be a potentially important antitumor target.

Understanding the nature of the binding interaction between the *N*-aryl-*N*-hydroxycarbamoyl esters of GSH and the active site of GlxI is clearly important, to provide a better basis for inhibitor design. Binding appears to result from two conceptually separate and distinct phenomena. First, the *N*-hydroxycarbamoyl ester function contributes to binding by modeling the stereoelectronic features of the tightly bound enediol intermediate and/or flanking transition states that form from the GSH–methylglyoxal–thiohemiacetal substrate, eq 1.⁹

Second, the *N*-aryl substituent also makes a major contribution to binding by interacting with a hydropho-

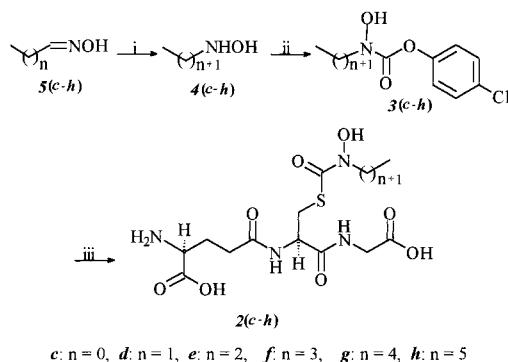
Chart 1. Structures of *S*-(*N*-Aryl-*N*-hydroxycarbamoyl)glutathiones **1a–d** and *S*-(*N*-Alkyl-*N*-hydroxycarbamoyl)glutathiones **2a–h**



bic pocket in the active site, as indicated by the increase in binding affinity with increasing hydrophobicity of the *N*-aryl substituent. The recently determined high-resolution X-ray crystal structure of the homodimeric human enzyme in complex with enediol analogue **1d** confirms the presence of a hydrophobic binding pocket in the active site.¹² In the structure, a catalytically essential active site Zn²⁺ directly coordinates both oxygen atoms of the syn-conformation of the *N*-hydroxy-

* To whom correspondence should be addressed. Tel: 410-455-2518. Fax: 410-455-2608. E-mail: creighto@umbc7.umbc.edu.

Scheme 1. Synthesis of *S*-(*N*-Alkyl-*N*-hydroxycarbamoyl)glutathiones **2c–h**^a



^a Reagents and conditions: (i) $(C_2H_5)_3SiH$; (ii) 4-chlorophenyl chloroformate; (iii) GSH/EtOH–H₂O, pH 9.

carbamoyl ester function, and the *N*-aryl substituent occupies a hydrophobic pocket composed of Phe 67A, Phe 62A, Leu 69A, Cys 60A, Phe 71A, Ile 88A, Leu 92A, Leu 174B, Leu 160B, Phe 162B, and Met 157B.

As part of a research program aimed at developing highly specific, tight-binding inhibitors of human GlxI, we have probed the dimensions and properties of the hydrophobic binding pocket using both experimental and computational methods. Essential to the conclusions of this study is a comparison of the inhibition constants of the *N*-aryl-*N*-hydroxycarbamoyl esters of GSH (**1a–c**) versus the homologous series of *N*-alkyl-*N*-hydroxycarbamoyl esters of GSH (**2a–h**) shown in Chart 1.

Chemistry and Enzymology

The *S*-(*N*-aryl-*N*-hydroxycarbamoyl)glutathione derivatives **1a–c** were prepared by reaction of GSH with the 4-chlorophenyl esters of the corresponding *N*-aryl-*N*-hydroxycarbamates, as previously described by this laboratory.⁹ *S*-(*N*-Hydroxycarbamoyl)glutathione (**2a**) was prepared by an acyl-interchange reaction between *N*-hydroxycarbamate 4-chlorophenyl ester (**3a**) and GSH. The acylating reagent (**3a**) was prepared by reacting hydroxylamine with 4-chlorophenyl chloroformate. *S*-(*N*-Hydroxy-*N*-methylcarbamoyl)glutathione (**2b**) was prepared by a published method from this laboratory.⁸ The *S*-(*N*-alkyl-*N*-hydroxycarbamoyl)glutathiones **2c–h** were synthesized as outlined in Scheme 1. The 4-chlorophenyl esters of the *N*-alkyl-*N*-hydroxycarbamates **3c–h** were prepared using a modification of the general method of Wu and Sun.¹³ In a one-pot reaction mixture, triethylsilane was first used to reduce the alkyl oximes **5c–h** to the corresponding hydroxylamines **4c–h**, followed by reaction with 4-chlorophenyl chloroformate to give **3c–h**. Reaction of GSH with **3c–h** gave crude preparations of **2c–h**, which were purified to apparent homogeneity by differential precipitation or reverse-phase HPLC. NMR spectral assignments were based on comparisons with previously published NMR studies of GSH and its derivatives.¹⁴

Human erythrocyte GlxI was purified to homogeneity from outdated human blood by a published procedure.¹⁵ *Pseudomonas putida* GlxI was purified from *Escherichia coli* BL21(DE3) transformed with pBTac1/GlxI,¹⁶ using methods described elsewhere.¹⁷

Table 1. Inhibition Constants (K_i 's) of *S*-(*N*-Aryl-*N*-hydroxycarbamoyl)glutathiones with Human Erythrocyte, Yeast, and *P. putida* GlxI^a

compd	π^b	K_i (μ M)		
		human ^c	yeast ^c	<i>P. putida</i>
2b	0.54	1.7 ± 0.1	68 ± 5	86 ± 9
1a	2.13	0.16 ± 0.1	11 ± 1	28 ± 3
1b	3.04	0.046 ± 0.004	3.6 ± 0.3	16 ± 1
1c	3.25	0.014 ± 0.001	1.2 ± 0.2	10 ± 2

^a Phosphate buffer (50 mM, pH 7), 25 °C. ^b Hansch hydrophobicity constants for R-substituents obtained from ref 20. ^c From ref 9.

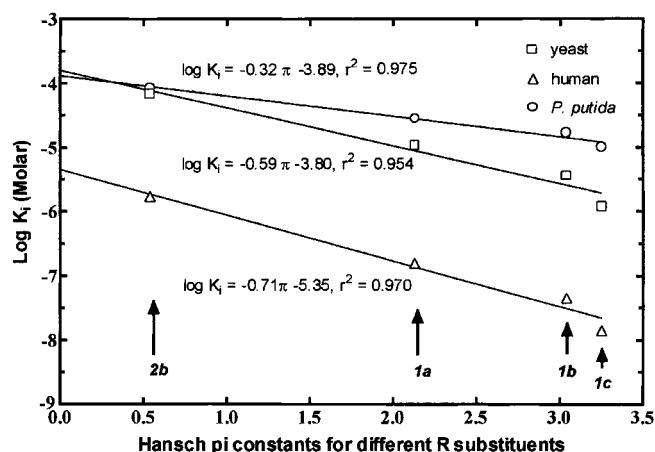


Figure 1. Log plot of competitive inhibition constants (K_i 's) versus the Hansch hydrophobicity constants of the R-substituents for *S*-(*N*-methyl-*N*-hydroxycarbamoyl)glutathione (**2b**) and different *S*-(*N*-aryl-*N*-hydroxycarbamoyl)glutathiones **1a–c** with human, yeast, and *P. putida* GlxI. The data for human and yeast GlxI were taken from ref 9.

Results and Discussion

The presence of a hydrophobic binding pocket in the active site of yeast GlxI was first suggested by Vince and co-workers, on the basis of the progressive decrease in the inhibition constants of simple *S*-aryl and *S*-alkyl GSH derivatives with increasing hydrophobicity of the *S*-substituent.¹⁸

Role of Hydrophobicity in Inhibitor Binding. Indeed, the binding affinities of the enediol analogues **2b** and **1a–c** for human, yeast, and *P. putida* GlxI increase with increasing hydrophobicity of the *N*-substituent (Table 1), indicated by the inverse relationship between $\log K_i$ and the hydrophobicity constants (π) of the *N*-methyl and *N*-aryl functions, Figure 1.¹⁹ The π constant is defined as the log of the *n*-octanol/water partition ratio for the *N*-aryl function, calculated according to the method of Hansch.²⁰ The slopes of the lines through the data measure the change in the free energy of transfer of the enediol analogues from aqueous buffer at pH 7 to the active sites of the enzymes relative to the change in the free energy of transfer of the analogues between buffer and *n*-octanol. Thus, the slopes for the yeast and human enzymes can be interpreted to indicate that the hydrophobicities of the respective binding pockets are about 60% and 70% that of *n*-octanol. The shallower slope for *P. putida* GlxI indicates a hydrophobicity about 30% that of *n*-octanol.

Polar/charged residues that are *not* present in the hydrophobic pockets of the human and yeast enzymes can explain the smaller apparent hydrophobicity of the

Table 2. Inhibition Constants (K_i 's) of *S*-(*N*-Alkyl-*N*-hydroxycarbamoyl)glutathiones with Human Erythrocyte GlxI^a

compd	π^b	K_i (μ M)	compd	π^b	K_i (μ M)
2a	0	183 \pm 50	2f	2.70	0.17 \pm 0.08
2c	1.08	1.18 \pm 0.07	2g	3.24	0.016 \pm 0.004
2d	1.62	0.80 \pm 0.5	2h	3.78	0.018 \pm 0.011
2e	2.16	0.18 \pm 0.09			

^a Phosphate buffer (100 mM, pH 7), 25 °C. ^b Hansch hydrophobicity constants for R-substituents calculated according to ref 20.

binding pocket in the bacterial enzyme. While there is no reported structural data for the yeast and bacterial enzymes, sequence comparisons with the human enzyme suggest the presence of analogous hydrophobic pockets in the active sites of the yeast and bacterial enzymes. In the human enzyme, Leu 92A and Ile 88A are 2 of 11 residues that compose the hydrophobic pocket identified in the X-ray crystal structure.²¹ These two residues are replaced, respectively, by Lys and His residues in the sequence of amino acids that comprise the apparent hydrophobic pocket in the bacterial enzyme, presumably resulting in a lower overall hydrophobicity. In contrast, Leu 92A and Ile 88A are conservatively replaced by two Phe residues in the yeast enzyme, consistent with the similar observed hydrophobicities for the yeast and human enzymes.

The binding affinities to human GlxI of a homologous series of *S*-(*N*-alkyl-*N*-hydroxycarbamoyl)glutathiones **2a–h** (Chart 1) were determined for comparison with those of the *N*-aryl derivatives, Table 2. Initially, we anticipated that the slope of the log K_i versus π plot would be shallower than that observed with the *N*-aryl derivatives (Figure 1), because of the increasing conformational flexibility of the *N*-alkyl function proceeding from *N*-methyl to *N*-heptyl. Conformational flexibility (entropy) should negatively impact binding affinity, if the active site binds only a limited subset of *N*-alkyl conformers that exist in bulk solvent. By one estimate, for each degree of rotational freedom lost upon binding of a ligand to a protein, there is roughly a 9-fold decrease in binding affinity.²² This effect will be less important proceeding from *N*-methyl to the *N*-aryl derivatives, as there is no systematic change in conformational flexibility of the *N*-substituent. However, contrary to expectation, the slopes for the two classes of compounds are identical within experimental error, Figure 2. This suggests either that there is little change in conformational flexibility of the *N*-alkyl derivatives upon binding to the enzyme or that there are compensating favorable enthalpic and/or entropic terms (due to solvent/protein reorganization), which are not reflected in the binding affinities of the *N*-aryl derivatives to the active site. In either case, conformational flexibility appears not to adversely affect the binding affinity of the *N*-alkyl enediol analogues with the active site of GlxI.

Role of Polar Interactions in Inhibitor Binding.

The intercept values on the log K_i axis of Figure 1 reflect the contribution of polar interactions to binding affinity. These values are the hypothetical inhibition constants for an enediol analogue in which the *N*-aryl function is replaced by *N*-H ($\pi = 0$), a functionality that cannot interact with the enzyme hydrophobically. The difference in the intercept values indicates that polar interactions make a 25-fold greater contribution to binding

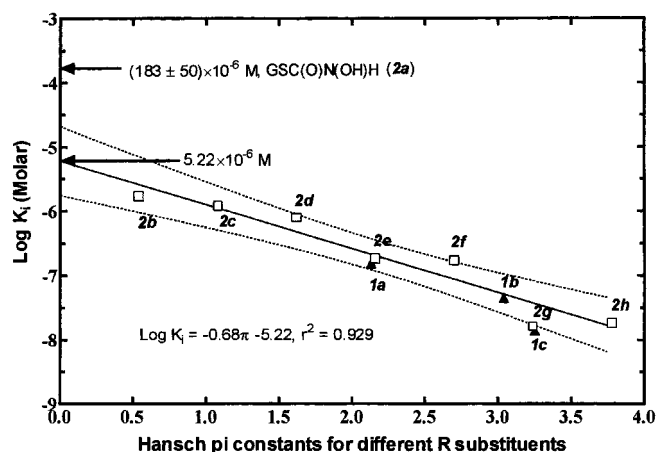


Figure 2. Log plot of competitive inhibition constants (K_i 's) versus the Hansch hydrophobicity constants of the R-substituents for *S*-(*N*-alkyl-*N*-hydroxycarbamoyl)glutathiones **2b–h** (\square) and *S*-(*N*-aryl-*N*-hydroxycarbamoyl)glutathiones **1a–c** (\blacktriangle) with human GlxI. The solid line is the result of linear regression analysis of the data for *S*-(*N*-alkyl-*N*-hydroxycarbamoyl)glutathiones. The dashed lines demarcate the 95% confidence interval. Also shown is the experimentally determined inhibition constant for *S*-(*N*-hydroxycarbamoyl)glutathione (**2a**).

affinity for the human enzyme than for the yeast and bacterial enzymes. Sequence comparisons indicate that one of the ligands (Gln 33) to the active site Zn^{2+} of the human enzyme is replaced by His in the yeast and bacterial enzymes.²¹ Conceivably, this might indirectly influence the stability of the direct coordination interaction between the Zn^{2+} and the *N*-hydroxycarbamoyl ester function of the bound enediol analogues. The difference in binding affinities is less easily explained by differential interactions with the glutathionyl moiety, as the active site residues that interact with the glutathionyl backbone of the bound inhibitors are strictly conserved among the enzymes from the three different biological sources.²¹

Of substantial interest is the observation that the experimentally measured value of the inhibition constant for *S*-(*N*-hydroxycarbamoyl)glutathione (**2a**, $K_i = 183 \mu\text{M}$) is 35-fold larger than the extrapolated value of $5.2 \mu\text{M}$ for this compound obtained from the intercept on the $\log K_i$ axis of the hydrophobicity plot of Figure 2. This strongly indicates that occupancy of the hydrophobic binding pocket somehow optimizes polar interactions between the enzyme and the bound ligand, perhaps by promoting alignments to the active site zinc ion. This is the first evidence for a cooperative relationship between the polar and hydrophobic interactions associated with binding an enediol analogue to the active site of GlxI.

Computational Studies. The binding of the *N*-aryl enediol analogues to the active site could be adversely affected by the presence of steric restrictions in the hydrophobic binding pocket. For example, the X-ray crystal structure of the binary GlxI·**1d** complex shows an orthogonal relationship between the plane of the phenyl ring and the plane of the *N*-hydroxycarbamoyl ester function.¹² The question of whether this might reflect steric bumping between the phenyl ring and active site residues was addressed using computational methods.

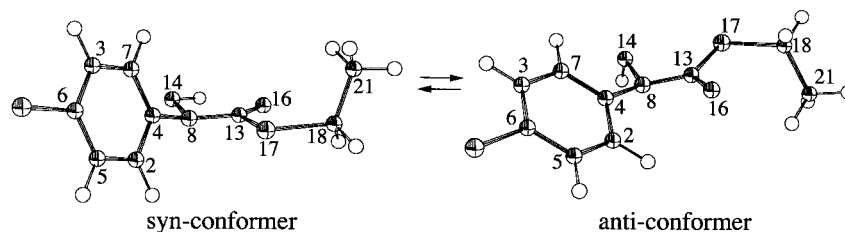


Figure 3. Geometry-optimized structures of the syn- and anti-conformations of *S*-(*N*-4-chlorophenyl-*N*-hydroxycarbamoyl)-thioethane. Critical dihedral angles are given in Table 3.

Table 3. Critical Dihedral Angles (deg) for the Geometry-Optimized Syn- and Anti-Conformers of *S*-(*N*-4-Chlorophenyl-*N*-hydroxycarbamoyl)thioethane (Figure 3) Obtained at the HF/6-31G*Level of Theory

bonds	syn-conformer	anti-conformer
C(2)–C(4)–N(8)–C(13)	–90.75	–56.27
C(2)–C(4)–N(8)–O(14)	122.76	156.48
C(7)–C(4)–N(8)–C(13)	90.78	125.49
C(7)–C(4)–N(8)–O(14)	–55.71	–21.77
C(4)–N(8)–C(13)–O(16)	–160.16	21.18
C(4)–N(8)–C(13)–S(17)	23.01	–161.26
O(14)–N(8)–C(13)–O(16)	–14.29	168.32
O(14)–N(8)–C(13)–S(17)	168.89	–14.13
relative energy (kcal/mol)	0	–3.4

The energy-minimized syn- and anti-conformers of the model compound, *S*-(*N*-4-chlorophenyl-*N*-hydroxycarbamoyl)thioethane, were calculated by both semiempirical and ab initio methods, Figure 3. The conformation of the *S*-substituent of the less stable syn-conformer is nearly identical to that of the *S*-substituent of the syn-conformer of **1d** observed in the X-ray crystal structure. At the Hartree–Fock/6-31G* level of theory, the dihedral angle between the plane of phenyl ring and that of the *N*-hydroxycarbamoyl ester function is 91°, which is close to that observed in the X-ray structure, Table 3. Apparently, the geometry of the ground-state structure of the model compound in the gas phase is determined largely by steric interactions between the ortho-protons of the ring and the *N*-OH and *S*-ethyl functions. By inference, human GlxI likely binds a low-energy conformer of syn-**1d** in which the *N*-aryl function is orthogonal to the plane of the *N*-hydroxycarbamoyl ester function. Thus, computational methods indicate that the conformation of the *S*-substituent of the enzyme-bound enediol analogue is a property of the ligand and not the result of steric interactions with the enzyme protein.

Implications for Catalysis and Inhibitor Design.

The inhibitor binding studies reported here indicate the presence of a large, diffuse hydrophobic binding pocket in the active site of human GlxI that plays a major role in binding the enediol analogues to the active site. Occupancy of this pocket is necessary in order to maximize polar interactions between the enzyme and bound enediol analogue. By inference, the methyl group of GSH–methylglyoxal thiohemiacetal substrate might participate in catalysis by helping to optimize interactions between active site residues and the enediol intermediate and flanking transition states. Each of these factors must be given careful consideration in the design of future mechanism-based competitive inhibitors of GlxI as potential antitumor agents.

Experimental and Computational Methods

Synthetic methods are outlined in Scheme 1. NMR spectra were taken on a GE QE-300 NMR spectrometer. Mass spectral data were obtained at the Midwest Center for Mass Spectrometry, University of Nebraska–Lincoln, and the Washington University Mass Spectrometry Resource, Washington University–Saint Louis. Elemental analyses were obtained at Atlantic Microlabs, Inc., Norcross, GA, and are within 0.4% of the calculated values unless otherwise indicated. Oximes **5c–h** were synthesized from the corresponding aldehydes by standard methods.²³ NMR and IR analyses of the oximes matched published standard spectra. All other reagents were purchased from Aldrich.

Competitive inhibition constants were calculated from the variation in the apparent K_m of GlxI with GSH–methylglyoxal–thiohemiacetal substrate in the presence of different concentrations of enediol analogue.⁹ Apparent K_m values were obtained from computer fits of the initial rate data to the Michaelis–Menten equation.

The lowest-energy gas-phase conformation of *S*-(*N*-4-chlorophenyl-*N*-hydroxycarbamoyl)thioethane was calculated using the molecular modeling program Spartan (Wavefunction, Inc., Irvine, CA).

***N*-Hydroxy-*N*-heptylcarbamate 4-Chlorophenyl Ester (3h).** This compound was prepared by a modification of a published method.²³ Heptanal oxime **5h** (1.0 g, 0.008 mol) was dissolved in 10 mL chloroform in a dry, nitrogen-flushed vessel on ice. Triethylsilane (0.90 g, 0.008 mol) was added dropwise, followed by dropwise addition of 4-chlorophenyl chloroformate (1.47 g, 0.008 mol). The mixture was stirred overnight under a nitrogen atmosphere at room temperature. The crude mixture was purified by flash gel chromatography, eluting with chloroform–methanol (40:1 to 30:1). The solvent was removed in vacuo to give a colorless oil, which crystallized to white needles on standing. The product was recrystallized from ether–hexane. Yield: 40%. Mp: 54 °C. 300 MHz ¹H NMR (CDCl₃, TMS): δ 0.86–0.90 (m, 3H), 1.27–1.32 (m, 8H), 1.67–1.72 (m, 2H), 1.78 (s, OH), 3.65 (t, *J* = 7.2 Hz, 2H), 7.06 (d, *J* = 8.7 Hz, aromatic-2H), 7.33 (d, *J* = 8.7 Hz, aromatic-2H). IR (KBr): 3250, 2920, 2840, 1670, 1480, 1420, 1220, 1160, 1080, 1010, 870, 810, 750 cm^{–1}. Anal. (C₁₄H₂₀ClNO₃) C, H, N.

***N*-Hydroxy-*N*-hexylcarbamate 4-Chlorophenyl Ester (3g).** This compound was prepared by the same general method used to prepare **3h**. The product was recrystallized from ether–hexane as colorless plates. Yield: 28%. Mp: 61–62 °C. 300 MHz ¹H NMR (CDCl₃, TMS): δ 0.86–0.91 (m, 3H), 1.2–1.4 (m, 8H), 1.6–1.8 (m, 2H), 3.66 (t, *J* = 7.2 Hz, 2H), 7.06 (d, *J* = 8.7 Hz, aromatic-2H), 7.33 (d, *J* = 8.7 Hz, aromatic-2H). IR (KBr): 3250, 2900, 2840, 1660, 1480, 1420, 1220, 1160, 1080, 1010, 870, 810, 750 cm^{–1}. Anal. (C₁₃H₁₈ClNO₃) C, H, N: calcd, 5.15; found, 5.08.

***N*-Hydroxy-*N*-pentylcarbamate 4-Chlorophenyl Ester (3f).** This compound was prepared by the same general method used to prepare **3h**. The product was recrystallized from ether–hexane as white rhomboidal crystals. Yield: 46%. Mp: 47–48 °C. 300 MHz ¹H NMR (CDCl₃, TMS): δ 0.91 (t, *J* = 6.6 Hz, 3H), 1.28–1.37 (m, 4H), 1.72 (m, 2H), 3.67 (t, *J* = 6.9 Hz, 2H), 6.66 (bs, OH), 7.07 (d, *J* = 8.7 Hz, aromatic-2H), 7.04 (d, *J* = 8.7 Hz, aromatic-2H). IR (KBr): 3250, 2920, 2845, 1660, 1480, 1420, 1210, 1160, 1080, 1005, 865, 810, 745 cm^{–1}. Anal. (C₁₂H₁₆ClNO₃) C, H, N: calcd, 5.43; found, 5.37.

N-Hydroxy-N-butylcarbamate 4-Chlorophenyl Ester (3e). This compound was prepared by the same general method used to prepare **3h**, using chloroform–ethyl acetate (100:1) as a chromatographic solvent. The product was recrystallized from ether–hexane as white flat needles. Yield: 23%. Mp: 42–43 °C. 300 MHz ^1H NMR (CDCl_3 , TMS): δ 0.93 (t, J = 7.2 Hz, 3H), 1.37 (m, 2H), 1.68 (m, 2H), 3.66 (t, J = 6.9 Hz, 2H), 7.2 (bs, OH), 7.06 (d, J = 8.7 Hz, aromatic-2H), 7.333 (d, J = 8.7 Hz, aromatic-2H). IR (KBr): 3250, 2920, 2850, 1640, 1460, 1400, 1260, 1190, 1130, 1050, 1020, 980, 845, 790, 725 cm^{-1} . Anal. ($\text{C}_{11}\text{H}_{14}\text{NClO}_3$) C; H: calcd, 5.79; found, 5.73; N: calcd, 5.75; found, 5.83.

N-Hydroxy-N-propylcarbamate 4-Chlorophenyl Ester (3d). This compound was prepared by the same general method used to prepare **3h**, using chloroform–ethyl acetate (100:1) as a chromatographic solvent. The product was crystallized from ether–hexane as colorless flat needles. Yield: 21%. Mp: 58–59 °C. 300 MHz ^1H NMR (CDCl_3 , TMS): δ 0.97 (t, J = 7.0 Hz, 3H), 1.76 (m, 2H), 3.64 (t, J = 7.0 Hz, 2H), 6.84 (bs, OH), 7.07 (d, J = 8.8 Hz, aromatic-2H), 7.33 (d, J = 8.8 Hz, aromatic-2H). IR (KBr): 3230, 2940, 2920, 2860, 1655, 1480, 1460, 1420, 1285, 1240, 1220, 1170, 1080, 1040, 1005, 865, 810, 745 cm^{-1} . Anal. ($\text{C}_{10}\text{H}_{12}\text{NClO}_3$) C; H: calcd, 5.27; found, 5.32; N: calcd, 6.10; found, 6.05.

N-Hydroxy-N-ethylcarbamate 4-Chlorophenyl Ester (3c). This compound was prepared by the same general method used to prepare **3h**, using chloroform–ethyl acetate (100:1) as a chromatographic solvent. The product was crystallized from ether–hexane as white needles. Yield: 16%. Mp: 67–68 °C. 300 MHz ^1H NMR (CDCl_3 , TMS): δ 1.31 (t, J = 7.0 Hz, 3H), 3.73 (t, J = 7.0 Hz, 2H), 6.40 (bs, OH), 7.08 (d, J = 8.8 Hz, aromatic-2H), 7.34 (d, J = 8.8 Hz, aromatic-2H). IR (KBr): 3250, 2970, 2910, 2880, 2860, 1665, 1480, 1425, 1270, 1220, 1170, 1080, 1030, 1005, 960, 865, 810, 745 cm^{-1} . Anal. ($\text{C}_9\text{H}_{10}\text{NClO}_3$) C; H: calcd, 4.67; found, 4.79; N: calcd, 6.50; found, 6.38.

N-Hydroxycarbamate 4-Chlorophenyl Ester (3a). This compound was prepared by reacting hydroxylamine with 4-chlorophenyl chloroformate. The product was crystallized from ether–hexane as colorless plates. Yield: 34%. Mp: 137–139 °C. 300 MHz ^1H NMR (CDCl_3 , TMS): δ 5.83 (bs, 1H), 7.11 (d, J = 8.7 Hz, 2H), 7.38 (d, J = 8.7 Hz, 2H), 7.47 (bs, 1H). IR (KBr): 3300, 1725, 1465, 1260, 1210, 1080, 1005, 840 cm^{-1} . Anal. ($\text{C}_7\text{H}_6\text{NClO}_3$) C; H: calcd, 3.22; found, 3.34; N: calcd, 7.47; found, 7.39.

S-(N-Heptyl-N-hydroxycarbamoyl)glutathione (2h). Into a stirring solution of 6.3 mL degassed, nitrogen-saturated ethanol:water (2:1) and **3h** (53 mg, 0.185 mmol) was placed a 6.3-fold excess of glutathione (563 mg, 1.16 mmol). The slurry was slowly brought to pH 9 by the dropwise addition of 6 N NaOH, during which the mixture became a homogeneous solution. The solution was placed under nitrogen and allowed to stand at room temperature for 24 h. The solution was brought to pH 3.5 with 6 N HCl and the solvent removed in vacuo. The white residue was suspended in 1 mL water, stirred for 9 h at room temperature, and the precipitate collected by centrifugation. This digestion procedure was repeated 4 more times. The dried white solid was then triturated 3 times with 0.8 mL portions of diethyl ether to remove unreacted **3h** and unreacted 4-chlorophenol. Yield: 35%. 300 MHz ^1H NMR (D_2O , pD 10.4, HOD reference): δ 0.88 (methyl-3H), 1.2–1.4 (m, alkyl-8H), 1.63 (m, alkyl-2H), 1.91 (m, Glu- C_βH_2), 2.40 (m, Glu- $\text{C}_\gamma\text{H}_2$), 3.07 (q, J = 9.0, 14.4 Hz, Cys- C_βH_a), 3.28 (q, J = 4.2, 14.4 Hz, Cys- C_βH_b), 3.32 (t, J = 6.0 Hz, Glu- C_αH), 3.59 (t, J = 6.6 Hz, N- CH_2), 3.75 (d, J = 17.1 Hz, Gly- $\text{C}_\alpha\text{H}_a$), 3.83 (d, J = 17.1 Hz, Gly- $\text{C}_\alpha\text{H}_b$), 4.53 (q, J = 4.2, 9.0 Hz, Cys- C_αH). FAB MS consistent with $\text{C}_{18}\text{H}_{32}\text{N}_4\text{SO}_8$. Anal. ($\text{C}_{18}\text{H}_{32}\text{N}_4\text{SO}_8$) C; H: calcd, 12.06; found, 11.92.

S-(N-Hexyl-N-hydroxycarbamoyl)glutathione (2g). This compound was prepared by the same general method used to prepare **2h**, using a reaction time of 70 h. Yield: 66%. 300 MHz ^1H NMR (D_2O , pD 10.4, DSS): δ 0.86 (methyl-3H), 1.28 (m, alkyl-6H), 1.60 (m, alkyl-2H), 1.87 (m, Glu- C_βH_2), 2.36 (m,

Glu- $\text{C}_\gamma\text{H}_2$), 3.04 (q, J = 9.0, 14.4 Hz, Cys- C_βH_b), 3.24 (q, J = 4.2, 14.4 Hz, Cys- C_βH_a), 3.27 (t, J = 6.6 Hz, Glu- C_αH), 3.57 (t, J = 6.9 Hz, N- CH_2), 3.72 (d, J = 17.1 Hz, Gly- $\text{C}_\alpha\text{H}_a$), 3.80 (d, J = 17.1 Hz, Gly- $\text{C}_\alpha\text{H}_b$), 4.50 (q, J = 4.2, 9.0 Hz, Cys- C_αH). FAB MS consistent with $\text{C}_{17}\text{H}_{30}\text{N}_4\text{SO}_8$. Anal. ($\text{C}_{17}\text{H}_{30}\text{N}_4\text{SO}_8$) C; H; N: calcd, 12.44; found, 12.28.

S-(N-Pentyl-N-hydroxycarbamoyl)glutathione (2f). This compound was prepared by the same general method used to prepare **2h**. Yield: 53%. 300 MHz ^1H NMR (D_2O , pD 10.4, DSS): δ 0.87 (methyl-3H), 1.28 (m, alkyl-4H), 1.61 (m, alkyl-2H), 1.91 (m, Glu- C_βH_2), 2.39 (m, Glu- $\text{C}_\gamma\text{H}_2$), 3.04 (q, J = 9.0, 14.4 Hz, Cys- C_βH_b), 3.26 (q, J = 4.2, 14.4 Hz, Cys- C_βH_a), 3.35 (t, J = 6.3 Hz, Glu- C_αH), 3.57 (t, J = 6.9 Hz, N- CH_2), 3.73 (d, J = 17.1 Hz, Gly- $\text{C}_\alpha\text{H}_a$), 3.80 (d, J = 17.1 Hz, Gly- $\text{C}_\alpha\text{H}_b$), 4.52 (q, J = 4.2, 9.0 Hz, Cys- C_αH). FAB MS consistent with $\text{C}_{16}\text{H}_{28}\text{N}_4\text{SO}_8$. Anal. ($\text{C}_{16}\text{H}_{28}\text{N}_4\text{SO}_8$) C; H: calcd, 6.47; found, 6.38; N: calcd, 12.84; found, 12.71.

S-(N-Butyl-N-hydroxycarbamoyl)glutathione (2e). This compound was prepared by the same general method used to prepare **2h**, using a reaction time of 115 h. The crude, acidified product was purified by flash chromatography on a silica gel column, using *n*-propanol:acetic acid:water (10:1:5) as an eluting solvent. The fractions containing the crude product were pooled, brought to dryness and further purified by reverse-phase column chromatography (Whatman μ Bondapak C_{18} , 0.78 \times 30 cm), using 0.25% acetic acid and 35% methanol in water as an eluting solvent (retention volume: \sim 26 mL). The peak fractions were lyophilized to dryness to give the final product as a white powder. Yield: 35%. 300 MHz ^1H NMR (D_2O , pD 3.3, DSS): δ 0.89 (t, J = 7.3 Hz methyl-3H), 1.28 (m, alkyl-2H), 1.59 (m, alkyl-2H), 2.15 (m, Glu- C_βH_2), 2.51 (m, Glu- $\text{C}_\gamma\text{H}_2$), 3.14 (q, J = 8.4, 14.3 Hz, Cys- C_βH_b), 3.37 (q, J = 4.8, 14.3 Hz, Cys- C_βH_a), 3.65 (t, J = 7.0 Hz, N- CH_2), 3.79 (t, J = 6.6 Hz, Glu- C_αH), 3.94 (s, Gly- $\text{C}_\alpha\text{H}_2$), 4.62 (q, J = 4.8, 8.4 Hz, Cys- C_αH). FAB MS consistent with $\text{C}_{15}\text{H}_{26}\text{N}_4\text{SO}_8$. Anal. ($\text{C}_{15}\text{H}_{26}\text{N}_4\text{SO}_8 \cdot \text{H}_2\text{O}$) C: calcd, 37.86; found, 37.46; H: calcd, 5.87; found, 5.76; N: calcd, 13.58; found, 13.26.

S-(N-Propyl-N-hydroxycarbamoyl)glutathione (2d). This compound was prepared by the same general method used to prepare **2e**. The flash chromatography column was eluted with *n*-propanol:acetic acid:water (70:25:30). The reverse-phase column was eluted with 0.25% acetic acid and 25% methanol in water (retention volume: \sim 23 mL). The peak fractions were lyophilized to dryness to give the final product as a white powder. Yield: 35%. 300 MHz ^1H NMR (D_2O , pD 3.3, DSS): δ 0.86 (t, J = 7.3 Hz, methyl-3H), 1.63 (m, J = 7.0, J = 7.3 alkyl-2H), 2.14 (m, Glu- C_βH_2), 2.51 (m, Glu- $\text{C}_\gamma\text{H}_2$), 3.12 (q, J = 8.4, 14.3 Hz, Cys- C_βH_b), 3.38 (q, J = 4.8, 14.3 Hz, Cys- C_βH_a), 3.61 (t, J = 7.0 Hz, N- CH_2), 3.79 (t, J = 6.2 Hz, Glu- C_αH), 3.94 (s, Gly- $\text{C}_\alpha\text{H}_2$), 4.62 (q, J = 4.8, 8.4 Hz, Cys- C_αH). FAB MS consistent with $\text{C}_{14}\text{H}_{24}\text{N}_4\text{SO}_8$. Anal. ($\text{C}_{14}\text{H}_{24}\text{N}_4\text{SO}_8 \cdot \text{H}_2\text{O}$) C; H: calcd, 6.15; found, 5.90; N: calcd, 6.50; found, 6.38.

S-(N-Ethyl-N-hydroxycarbamoyl)glutathione (2c). This compound was prepared by the same general method used to prepare **2e**. The flash chromatography column was eluted with *n*-propanol:acetic acid:water (130:1:70). The reverse-phase column was eluted with 0.25% acetic acid and 5% methanol in water (retention volume: \sim 24 mL). The peak fractions were lyophilized to dryness to give the final product as a white powder. Yield: 48%. 300 MHz ^1H NMR (D_2O , pD 3.3, DSS): δ 1.16 (t, J = 7.0 Hz, methyl-3H), 2.15 (m, Glu- C_βH_2), 2.51 (m, Glu- $\text{C}_\gamma\text{H}_2$), 3.12 (q, J = 8.4, 14.3 Hz, Cys- C_βH_b), 3.38 (q, J = 4.8, 14.3 Hz, Cys- C_βH_a), 3.66 (t, J = 7.0 Hz, N- CH_2), 3.79 (t, J = 6.2 Hz, Glu- C_αH), 3.94 (s, Gly- $\text{C}_\alpha\text{H}_2$), 4.63 (q, J = 4.8, 8.4 Hz, Cys- C_αH). FAB MS consistent with $\text{C}_{13}\text{H}_{22}\text{N}_4\text{SO}_8$. Anal. ($\text{C}_{13}\text{H}_{22}\text{N}_4\text{SO}_8 \cdot \text{H}_2\text{O}$) C: calcd, 37.86; found, 37.46; H: calcd, 5.87; found, 5.76; N: calcd, 13.58; found, 13.26.

S-(N-Hydroxycarbamoyl)glutathione (2a). This compound was prepared by the same general method used to prepare **2h**, using a 3.5-fold excess of GSH and a reaction time of 4 h. The crude reaction mixture was treated with 4-pyridine disulfide in order derivatize any unreacted GSH to the mixed

disulfide. This allowed a clean separation of the desired product by reverse-phase column chromatography using 0.25% acetic acid in water (retention volume: ~16 mL). The peak fractions were lyophilized to dryness to give the final product as a white powder. Yield: 30%. 300 MHz ^1H NMR (D_2O , pD 3.2, DSS): δ 2.15 (m, Glu- C_βH_2), 2.51 (m, Glu- $\text{C}_\gamma\text{H}_2$), 3.20 (q, $J = 8.1$, 14.3 Hz, Cys- C_βH_b), 3.43 (q, $J = 4.8$, 14.3 Hz, Cys- C_βH_a), 3.81 (t, $J = 6.2$ Hz, Glu- C_αH), 3.95 (s, Gly- $\text{C}_\alpha\text{H}_2$), 4.66 (q, $J = 4.8$, 8.1 Hz, Cys- C_αH). FAB MS consistent with $\text{C}_{11}\text{H}_{18}\text{N}_4\text{SO}_8$. Anal. ($\text{C}_{11}\text{H}_{18}\text{N}_4\text{SO}_8 \cdot \text{H}_2\text{O}$) C; H: calcd, 5.24; found, 5.17; N: calcd, 14.58; found, 14.36.

Acknowledgment. This work was supported by grants from the National Cancer Institute (CA 59612) and the U.S. Army Medical Research and Materiel Command.

References

- Thornalley, P. J. Glutathione-Dependent Detoxification of Alpha-Oxoaldehydes by the Glyoxalase System: Involvement in Disease Mechanisms and Antiproliferative Activity of Glyoxalase I Inhibitors. *Chem. Biol. Interact.* **1998**, *111–112*, 137–151.
- Creighton, D. J.; Hamilton, D. S.; Kavarana, M. J.; Sharkey, E. M.; Eiseman, J. L. Glyoxalase Enzyme System as a Potential Target for Antitumor Drug Development. *Drugs Future* **2000**, *25*, 385–392.
- Vander Jagt, D. L. The Glyoxalase System. In *Coenzymes and Cofactors: Glutathione*; Dolphin, D., Poulson, R., Avramovic, O., Eds.; John Wiley and Sons: New York, 1989; Vol. 3 (Part A), pp 597–641.
- Creighton, D. J.; Pourmotabbed, T. Glutathione-Dependent Aldehyde Oxidation Reactions. In *Molecular Structure and Energetics: Principles of Enzyme Activity*; Liebman, J. F., Greenberg, A., Eds.; VCH Publishers: New York, 1988; Vol. 9, pp 353–386.
- Richard, J. P. Kinetic Parameters for the Elimination Reaction Catalyzed by Triosephosphate Isomerase and an Estimation of the Reaction's Physiological Significance. *Biochemistry* **1991**, *30*, 4581–4585.
- White, J. S.; Rees, K. R. Inhibitory Effects of Methylglyoxal on DNA, RNA and Protein Synthesis in Cultured Guinea Pig Keratinocytes. *Chem. Biol. Interact.* **1982**, *38*, 339–347.
- Papoulis, A.; Al-Abed, Y.; Bucala, R. Identification of N^2 -(1-Carboxyethyl)guanine (CEG) as a Guanine Advanced Glycation End Product. *Biochemistry* **1995**, *34*, 648–655.
- Hamilton, D. S.; Creighton, D. J. Inhibition of Glyoxalase I by the Enediol Mimic *S*-(*N*-Hydroxy-*N*-methylcarbamoyl)glutathione: the Possible Basis of a Tumor-Selective Anticancer Strategy. *J. Biol. Chem.* **1992**, *267*, 24933–24936.
- Murthy, N. S. R. K.; Bakeris, T.; Kavarana, M. J.; Hamilton, D. S.; Lan, Y.; Creighton, D. J. *S*-(*N*-Aryl-*N*-hydroxycarbamoyl)-glutathione Derivatives are Tight-Binding Inhibitors of Glyoxalase I and Slow Substrates for Glyoxalase II. *J. Med. Chem.* **1994**, *37*, 2161–2166.
- Kavarana, M. J.; Kovaleva, E. G.; Creighton, D. J.; Wollman, M. B.; Eiseman, J. L. Mechanism-Based Competitive Inhibitors of Glyoxalase I: Intracellular Delivery, In Vitro Antitumor Activities, and Stabilities in Human Serum and Mouse Serum. *J. Med. Chem.* **1999**, *42*, 221–228.
- Sharkey, E. M.; O'Neill, H. B.; Kavarana, M. J.; Wang, H.; Creighton, D. J.; Sentz, D. L.; Eiseman, J. L. Pharmacokinetics and Antitumor Properties in Tumor-bearing Mice of an Enediol Analogue Inhibitor of Glyoxalase I. *Cancer Chemother. Pharmacol.* **2000**, *46*, 156–166.
- Cameron, A. D.; Ridderstrom, M.; Olin, B.; Kavarana, M. J.; Creighton, D. J.; Mannervik, B. Reaction Mechanism of Glyoxalase I Explored by an X-ray Crystallographic Analysis of the Human Enzyme in Complex with a Transition State Analogue. *Biochemistry* **1999**, *38*, 13480–13490.
- Wu, P.-L.; Sun, C.-J. A Simple Method for the Preparation of *N*-Substituted Hydroxamic Acids by Reductive Acylation of Oximes. *Tetrahedron Lett.* **1991**, *32*, 4137–4138.
- Rabenstein, D. L.; Keire, D. A. The Glyoxalase System. In *Coenzymes and Cofactors: Glutathione*; Dolphin, D., Poulson, R., Avramovic, O., Eds.; John Wiley and Sons: New York, 1989; Vol. 3 (Part A), pp 67–101.
- Aronsson, A.-C.; Tibbelin, G.; Mannervik, B. Purification of Glyoxalase I from Human Erythrocytes by the Use of Affinity Chromatography and Separation of Three Isozymes. *Anal. Biochem.* **1979**, *92*, 390–393.
- Lu, T.; Creighton, D. J.; Antoine, M.; Fenselau, C.; Lovett, P. S. The Gene Encoding Glyoxalase I from *Pseudomonas putida*: Cloning, Overexpression, and Sequence Comparisons with Human Glyoxalase I. *Gene* **1994**, *150*, 93–96.
- Rhee, H.-I.; Murata, K.; Kimura, A. Purification and Characterization of Glyoxalase I from *Pseudomonas putida*. *Biochem. Biophys. Res. Commun.* **1986**, *141*, 993–999.
- Vince, R.; Daluge, S.; Wadd, W. Studies on the Inhibition of Glyoxalase I by *S*-Substituted Glutathiones. *J. Med. Chem.* **1971**, *14*, 402–405.
- Electronic effects appear to have little influence on binding affinity. The greater electron-withdrawing ability of the para-substituted *N*-aryl substituents, relative to the *N*-methyl function, would be expected to decrease the stability of the direct coordination interaction between the active site Zn^{2+} and the *N*-hydroxycarbamoyl ester function of the bound ligands. If this were a major factor in binding affinity, the *N*-aryl enediol analogues should bind less tightly to the enzyme than the *N*-methyl enediol analogue, contrary to observation. Electronic effects on binding of the *N*-aryl enediol analogues to the enzyme are probably small because the X-ray structure of the binary GlxI-1d complex shows that the plane of the *N*-aryl function is orthogonal to the plane of the *N*-hydroxycarbamoyl function. This would effectively eliminate resonance effects on the distribution of charge in the *N*-hydroxycarbamoyl ester function.
- Hansch, C.; Kim, K. W.; Sarma, R. H. Structure-Activity Relationship in Benzamides Inhibiting Alcohol Dehydrogenase. *J. Am. Chem. Soc.* **1973**, *95*, 6447–6449.
- Cameron, A. D.; Olin, B.; Ridderstrom, M.; Mannervik, B.; Jones, A. Crystal Structure of Human Glyoxalase I – Evidence for Gene Duplication and 3D Domain Swapping. *EMBO* **1997**, *16*, 3386–3395.
- Page, I. M.; Jencks, W. P. Entropic Contributions to Rate Accelerations in Enzymic and Intramolecular Reactions and the Chelate Effect. *Proc. Natl. Acad. Sci. U.S.A.* **1971**, *68*, 1678–1683.
- Sandler, S. R.; Karo, W. *Organic Functional Group Preparations*; Academic Press: New York, 1972; Vol. III, Chapter 11.

JM000160L